1 Nuclear fusion reactions

Most of this book is devoted to the physical principles of energy production by fusion reactions in an inertially confined medium. To begin with, in this chapter we briefly discuss fusion reactions.

We first define fusion cross section and reactivity, and then present and justify qualitatively the standard parametrization of these two important quantities. Next, we consider a few important fusion reactions, and provide expressions, data, and graphs for the evaluation of their cross sections and reactivities. These results will be used in the following chapters to derive the basic requirements for fusion energy production, as well as to study fusion ignition and burn in suitable inertially confined *fuels*.

In the last part of this chapter, we also briefly discuss how high material density and spin polarization affect fusion reactivities. Finally, we outline the principles of muon-catalysed fusion.

1.1 | **Exothermic nuclear reactions: fission and fusion**

According to Einstein's mass–energy relationship, a nuclear reaction in which the total mass of the final products is smaller than that of the reacting nuclei is exothermic, that is, releases an energy

Reaction Q

$$Q = \left(\sum_i m_i - \sum_f m_f \right) c^2 \qquad 1.1$$

proportional to such a mass difference. Here the symbol m denotes mass, the subscripts i and f indicate, respectively, the initial and the final products, and c is the speed of light. We can identify exothermic reactions by considering the masses and the binding energies of each of the involved nuclei. The mass m of a nucleus with atomic number Z and mass number A differs from the sum of the masses of the Z protons and $A - Z$ neutrons, which build up the nucleus by a quantity

$$\Delta m = Z m_p + (A - Z) m_n - m. \qquad 1.2$$

Here m_p and m_n are the mass of the proton and of the neutron, respectively. For stable nuclei Δm is positive, and one has to provide an amount of energy equal to the binding energy

Nucleus binding energy

$$B = \Delta m c^2 \qquad 1.3$$

in order to dissociate the nucleus into its component neutrons and protons.

The Q value of a nuclear reaction can then be written as the difference between the final and the initial binding energies of the interacting nuclei:

Q and binding energy

$$Q = \sum_f B_f - \sum_i B_i. \qquad 1.4$$

Accurate data on nuclear masses and binding energies have been published by Audi and Wapstra (1995). A particularly useful quantity is the average binding energy per nucleon B/A, which is plotted in Fig. 1.1 as a function of the mass number A. We see that B/A, which is zero for $A = 1$, that is, for the hydrogen nucleus, grows rapidly with A, reaches a broad maximum of 8.7 MeV about $A = 56$ and then decreases slightly. For the heaviest nuclei $B/A \cong 7.5$ MeV. Notice the particularly high value of B/A for ^{4}He nucleus (the α-particle). The symbols D and T indicate, as usual, deuterium and tritium, that is, the hydrogen isotopes with mass two and three, respectively. According to the above discussion, exothermic reactions occur when the final reaction products have larger B/A than the reacting nuclei. As indicated in Fig. 1.1, this occurs for fission reactions, in which a heavy nucleus is split into lighter fragments, and for fusion reactions, in which two light nuclei merge to form a heavier nucleus.

Fission vs fusion

Fig. 1.1 Binding energy per nucleon versus mass number A, for the most stable isobars. For $A = 3$ also the unstable tritium is included, in view of its importance for controlled fusion. Notice that the mass number scale is logarithmic in the range 1–50 and linear in the range 50–250.
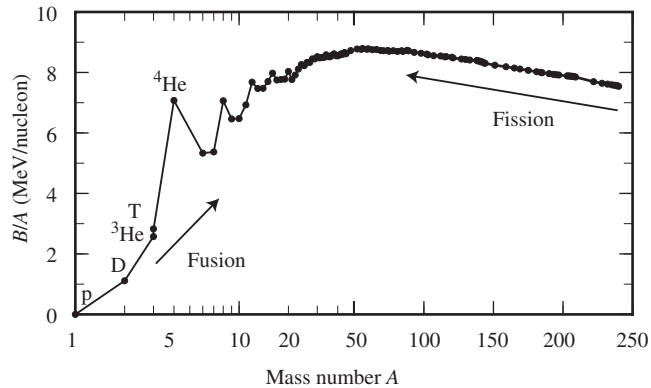
1.2 Fusion reaction physics

In most fusion reactions two nuclei (X_1 and X_2) merge to form a heavier nucleus (X_3) and a lighter particle (X_4). To express this, we shall use either of the equivalent standard notations

$$X_1 + X_2 \rightarrow X_3 + X_4, \qquad\qquad 1.5$$

or

$$X_1(x_2, x_4)X_3. \qquad\qquad 1.6$$

Due to conservation of energy and momentum, the energy released by the reaction is distributed among the two fusion products in quantity inversely proportional to their masses.

We indicate the velocities of the reacting nuclei in the laboratory system with $\mathbf{v}_1$ and $\mathbf{v}_2$, respectively, and their relative velocity with $\mathbf{v} = \mathbf{v}_1 - \mathbf{v}_2$. The center-of-mass energy of the system of the reacting nuclei is then

$$\epsilon = \tfrac{1}{2}m_\mathrm{r}v^2, \qquad\qquad 1.7$$

where $v = |\mathbf{v}|$, and

$$m_\mathrm{r} = \frac{m_1 m_2}{m_1 + m_2} \qquad\qquad 1.8$$

is the reduced mass of the system.

1.2.1 Cross section, reactivity, and reaction rate

Cross section

A most important quantity for the analysis of nuclear reactions is the *cross section*, which measures the probability per pair of particles for the

occurrence of the reaction. To be more specific, let us consider a uniform beam of particles of type '1', with velocity v_1, interacting with a target containing particles of type '2' at rest. The cross section $\sigma_{12}(v_1)$ is defined as the number of reactions per target nucleus per unit time when the target is hit by a unit flux of projectile particles, that is, by one particle per unit target area per unit time. Actually, the above definition applies in general to particles with relative velocity v, and is therefore symmetric in the two particles, since we have $\sigma_{12}(v) = \sigma_{21}(v)$.

Cross sections can also be expressed in terms of the centre-of-mass energy 1.7, and we have $\sigma_{12}(\epsilon) = \sigma_{21}(\epsilon)$. In most cases, however, the cross sections are measured in experiments in which a beam of particles with energy ϵ_1, measured in the laboratory frame, hits a target at rest. The corresponding beam-target cross-section $\sigma_{12}^{\text{bt}}(\epsilon_1)$ is related to the centre-of-mass cross-section $\sigma_{12}(\epsilon)$ by

Beam-target and centre-of-mass cross section

$$\sigma_{12}(\epsilon) = \sigma_{12}^{\text{bt}}(\epsilon_1), \qquad\qquad 1.9$$

with $\epsilon_1 = \epsilon \cdot (m_1 + m_2)/m_2$. From now on, we shall refer to centre-of-mass cross-sections and omit the indices 1 and 2.

If the target nuclei have density n_2 and are at rest or all move with the same velocity, and the relative velocity is the same for all pairs of projectile–target nuclei, then the probability of reaction of nucleus '1' per unit path is given by the product $n_2\sigma(v)$. The probability of reaction per unit time is obtained by multiplying the probability per unit path times the distance v travelled in the unit time, which gives $n_2\sigma(v)v$.

Another important quantity is the *reactivity*, defined as the probability of reaction per unit time per unit density of target nuclei. In the present simple case, it is just given by the product σv. In general, target nuclei move, so that the relative velocity v is different for each pair of interacting nuclei. In this case, we compute an *averaged reactivity*

Averaged reactivity

$$\langle \sigma v \rangle = \int_0^\infty \sigma(v) v f(v)\, dv, \qquad\qquad 1.10$$

where $f(v)$ is the distribution function of the relative velocities, normalized in such a way that $\int_0^\infty f(v)\, dv = 1$. It is to be observed that when projectile and target particles are of the same species, each reaction is counted twice.

Both controlled fusion fuels and stellar media are usually mixtures of elements where species '1' and '2', have number densities n_1 and n_2, respectively. The volumetric *reaction rate*, that is, the number of reactions per unit time and per unit volume is then given by

Volumetric reaction rate

$$R_{12} = \frac{n_1 n_2}{1 + \delta_{12}} \langle \sigma v \rangle = \frac{f_1 f_2}{1 + \delta_{12}} n^2 \langle \sigma v \rangle. \qquad\qquad 1.11$$

Here n is the total nuclei number density and f_1 and f_2 are the atomic fractions of species '1' and '2', respectively. The Kronecker symbol δ_{ij} (with $\delta_{ij} = 1$, if $i = j$ and $\delta_{ij} = 0$ elsewhere) is introduced to properly take

into account the case of reactions between like particles. Equation 1.11 shows a very important feature for fusion energy research: the volumetric reaction rate is proportional to the square of the density of the mixture. For future reference, it is also useful to recast it in terms of the mass density ρ of the reacting fuel

The reaction rate is proportional to the square of the density

$$R_{12} = \frac{f_1 f_2}{1 + \delta_{12}} \frac{\rho^2}{\bar{m}^2} \langle \sigma v \rangle, \qquad\qquad 1.12$$

where $\bar{m}$ is the average nuclear mass. Here, the mass density is computed as $\rho = \sum_j n_j m_j = n\bar{m}$, where the sum is over all species, and the very small contribution due to the electrons is neglected. We also immediately see that the specific reaction rate, that is, the reaction rate per unit mass, is proportional to the mass density, again indicating the role of the density of the fuel in achieving efficient release of fusion energy.

1.2.2 Fusion cross section parametrization

In order to fuse, two positively charged nuclei must come into contact, winning the repulsive Coulomb force. Such a situation is made evident by the graph of the radial behaviour of the potential energy of a two nucleon system, shown in Fig. 1.2. The potential is essentially Coulombian and repulsive,

$$V_c(r) = \frac{Z_1 Z_2 e^2}{r}, \qquad\qquad 1.13$$

at distances greater than

$$r_n \cong 1.44 \times 10^{-13}(A_1^{1/3} + A_2^{1/3}) \ \text{cm}, \qquad\qquad 1.14$$

which is about the sum of the radii of the two nuclei. In the above equations Z_1 and Z_2 are the atomic numbers, A_1 and A_2 the mass numbers of the
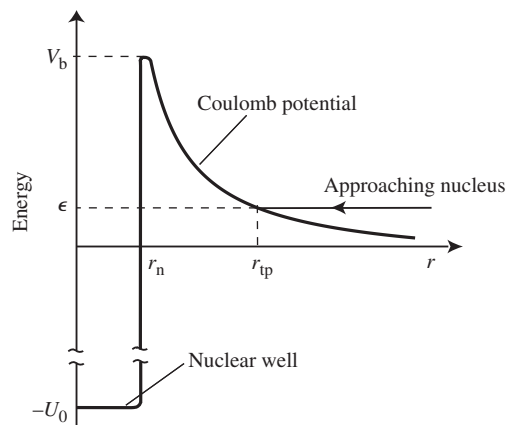

Fig. 1.2 Potential energy versus distance between two charged nuclei approaching each other with center-of-mass energy ϵ. The figure shows the nuclear well, the Coulomb barrier, and the classical turning point.

interacting nuclei, and e is the electron charge. At distances $r < r_\mathrm{n}$ the two nuclei feel the attractive nuclear force, characterized by a potential well of depth $U_0 = 30$–40 MeV.

Using eqns 1.13 and 1.14 we find that the height of the Coulomb barrier

Coulomb barrier

$$V_\mathrm{b} \simeq V_\mathrm{c}(r_\mathrm{n}) = \frac{Z_1 Z_2}{A_1^{1/3} + A_2^{1/3}} \ \ \text{MeV} \qquad 1.15$$

is of the order of one million electron-volts (1 MeV). According to classical mechanics, only nuclei with energy exceeding such a value can overcome the barrier and come into contact. Instead, two nuclei with relative energy $\epsilon < V_\mathrm{b}$ can only approach each other up to the classical turning point

$$r_\mathrm{tp} = \frac{Z_1 Z_2 e^2}{\epsilon}. \qquad 1.16$$

Quantum mechanics, however, allows for *tunnelling* a potential barrier of finite extension, thus making fusion reactions between nuclei with energy smaller than the height of the barrier possible.

Fusion reactions rely on tunnelling

A widely used parametrization of fusion reaction cross-sections is

$$\sigma \approx \sigma_\mathrm{geom} \times \mathcal{T} \times \mathcal{R}, \qquad 1.17$$

where σ_geom is a geometrical cross-section, $\mathcal{T}$ is the barrier transparency, and $\mathcal{R}$ is the probability that nuclei come into contact fuse. The first quantity is of the order of the square of the de-Broglie wavelength of the system:

$$\sigma_\mathrm{geom} \approx \lambdabar^2 = \left(\frac{\hbar}{m_\mathrm{r} v}\right)^2 \propto \frac{1}{\epsilon}, \qquad 1.18$$

where $\hbar$ is the reduced Planck constant and m_r is the reduced mass 1.8. Concerning the barrier transparency, we shall see that it is often well approximated by

Barrier transparency

$$\mathcal{T} \approx \mathcal{T}_\mathrm{G} = \exp(-\sqrt{\epsilon_\mathrm{G}/\epsilon}), \qquad 1.19$$

which is known as the Gamow factor (after the scientist who first computed it), where

Gamow energy

$$\epsilon_\mathrm{G} = (\pi \alpha_\mathrm{f} Z_1 Z_2)^2 2 m_\mathrm{r} c^2 = 986.1 Z_1^2 Z_2^2 A_\mathrm{r} \ \ \text{keV} \qquad 1.20$$

is the Gamow energy, $\alpha_\mathrm{f} = e^2/\hbar c = 1/137.04$ is the fine-structure constant commonly used in quantum mechanics, and $A_\mathrm{r} = m_\mathrm{r}/m_\mathrm{p}$. Equation 1.19 holds as far as $\epsilon \ll \epsilon_\mathrm{G}$, which sets no limitations to the problems we are interested in. Equations 1.19 and 1.20 show that the chance of tunnelling decreases rapidly with the atomic number and mass, thus providing a first simple explanation for the fact that fusion reactions of interest for energy production on earth only involve the lightest nuclei.

The *reaction characteristics* $\mathcal{R}$ contains essentially all the nuclear physics of the specific reaction. It takes substantially different values depending on the nature of the interaction characterizing the reaction. It is largest for reactions due to strong nuclear interactions; it is smaller by several orders of magnitude for electromagnetic nuclear interactions; it is still smaller by as many as 20 orders of magnitude for weak interactions. For most reactions, the variation of $\mathcal{R}(\epsilon)$ is small compared to the strong variation due to the Gamow factor.

In conclusion, the cross section is often written as

$$\sigma(\epsilon) = \frac{S(\epsilon)}{\epsilon} \exp(-\sqrt{\epsilon_G/\epsilon}), \qquad\qquad 1.21$$

Astrophysical S factor

where the function $S(\epsilon)$ is called the *astrophysical S factor*, which for many important reactions is a weakly varying function of the energy.

An excellent introduction to the computation of fusion cross-sections and thermonuclear reaction rates can be found in the classical textbook on stellar nucleosynthesis by Clayton (1983). Classic references on nuclear physics are Blatt and Weisskopf (1953), Segrè (1964), and Burcham (1973). In the following portion of this section, we outline the evaluation of the fusion cross-section for non-resonant reactions, which justifies the parametrization 1.21. The treatment is simplified and qualitative, but still rather technical. The reader not interested in such details can skip Section 1.2.3 without loss of the comprehension of the rest of the chapter.

1.2.3   Penetration factors for non-resonant reactions

The total cross-section can be obtained as a sum over partial waves, that is over the contributions of the different terms of an expansion of the particle wave-function in the components of the angular momentum l. We then write

Partial wave expansion

$$\sigma(v) = \sum_l \sigma_l(v), \qquad\qquad 1.22$$

Far from resonances the partial cross-section can be put in the form:

$$\sigma_l(v) \approx 2\pi \lambdabar^2 (2l + 1)\beta_l \mathcal{T}_l, \qquad\qquad 1.23$$

where β_l is a function taking into account nuclear interactions and $\mathcal{T}_l$ is the barrier transmission coefficient. This last factor, defined as the ratio of particles entering the nucleus per unit time to the number of particles incident on the barrier per unit time, can be written as

$$\mathcal{T}_l \approx P_l \left(1 + \frac{\lambdabar^2}{\lambdabar_0^2}\right)^{-1/2} = P_l \left(1 + \frac{U_0}{\epsilon}\right)^{-1/2} \approx \left(\frac{\epsilon}{U_0}\right)^{1/2} P_l, \quad 1.24$$

that is, the product of the barrier penetration factor P_l, measuring the probability that nucleus '2' reaches the surface of nucleus '1', and of

a potential discontinuity factor, due to the difference between the wavelength of the free nucleus and that of the compound nucleus in the nuclear well $\lambda_0 = \hbar/(2m_{\mathrm{r}}U_0)^{1/2}$. According to quantum mechanics, the barrier penetration factors P_l are computed by solving the time-independent Schroedinger equation

$$\frac{\hbar^2}{2m_{\mathrm{r}}}\nabla^2\psi + (\epsilon - V_{\mathrm{c}})\psi = 0 \qquad\qquad 1.25$$

for the wavefunction $\psi(\mathbf{r})$ describing the relative motion of the two interacting nucleons in a Coulomb potential extending from $r = 0$ to infinity. As usual for problems characterized by a central potential, we separate radial and angular variables, that is, we write $\psi(r,\theta,\phi) = Y(\theta,\phi)\chi(r)/r$. We then expand the function $\chi(r)$ into angular momentum components, $\chi_l(r)$, each satisfying the equation

$$\frac{d^2}{dr^2}\chi_l(r) + \frac{2m_{\mathrm{r}}}{\hbar^2}\left[\epsilon - W_l(r)\right]\chi_l(r) = 0, \qquad\qquad 1.26$$

where

Potential for *l*-th wave

$$W_l(r) = V_{\mathrm{c}}(r) + \frac{\hbar^2 l(l+1)}{2m_{\mathrm{r}}r^2} \qquad\qquad 1.27$$

takes the role of an effective potential for the lth component. This last equation shows that each angular momentum component sees an effective potential barrier of height increasing with l. We therefore expect the $l = 0$ component (S-wave) to dominate the cross section, in particular for light elements. An exception will occur for reactions in which the compound nucleus, formed when the two nuclei come into contact, has forbidden $l = 0$ levels. This latter case, however, does not occur for any reaction of relevance to controlled fusion.

Once the solution $\chi_l(r)$ of eqn 1.26 is known, the penetration factor for particles with angular momentum l is given by

$$P_l = \frac{\chi_l^*(r_{\mathrm{n}})\chi_l(r_{\mathrm{n}})}{\chi_l^*(\infty)\chi_l(\infty)}. \qquad\qquad 1.28$$

Penetration factors from WKB method

Exact computations of the wavefunctions $\chi_l(r)$ are feasible, but involved (Bloch *et al.* 1951). However, much simpler and yet accurate evaluations of the penetration factors can be performed by means of WKB method (after the initials of Wentzel, Kramers, and Brillouin), discussed in detail in standard books on quantum mechanics (Landau and Lifshitz 1965; Messiah 1999) or mathematical physics (Matthews and Walker 1970). A pedagogical application to the computation of

penetration factors is presented by Clayton (1983). Here it suffices to say that application of the method leads to

$$P_l = \left[\frac{W_l(r_n) - \epsilon}{\epsilon} \right]^{1/2} \exp(-G_l), \qquad 1.29$$

with the dominant exponential factor given by

$$G_l = 2 \frac{(2m_r)^{1/2}}{\hbar} \int_{r_n}^{r_{tp}(\epsilon)} [W_l(r) - \epsilon]^{1/2} \, dr, \qquad 1.30$$

where r_{tp} is the turning point distance 1.16. For $l = 0$, using eqn 1.27 for $W_l(r)$, we get

$$G_0 = \frac{2}{\pi} \sqrt{\frac{\epsilon_G}{\epsilon}} \left[\arccos \sqrt{\frac{r_n}{r_{tp}}} - \sqrt{\frac{r_n}{r_{tp}}} \sqrt{1 - \frac{r_n}{r_{tp}}} \right]. \qquad 1.31$$

Since for eqns 1.15 and 1.16, $r_n/r_{tp}(\epsilon) = \epsilon/V_b$, and in the cases of interest $\epsilon \ll V_b$, we can expand the right-hand side of eqn 1.31 in powers of (ϵ/V_b), thus obtaining

$$G_0 = \sqrt{\frac{\epsilon_G}{\epsilon}} \left[1 - \frac{4}{\pi} \left(\frac{\epsilon}{V_b} \right)^{1/2} + \frac{2}{3\pi} \left(\frac{\epsilon}{V_b} \right)^{3/2} + \cdots \right]. \qquad 1.32$$

In the low energy limit, we have $G_0 \simeq (\epsilon_G/\epsilon)^{1/2}$, and the S-wave penetration factor becomes

$$P_0 \simeq \left(\frac{V_b}{\epsilon} \right)^{1/2} \exp \left(-\sqrt{\frac{\epsilon_G}{\epsilon}} \right). \qquad 1.33$$

Penetration factors for $l > 0$ are approximately given by

$$P_l = P_0 \exp \left[-2l(l+1) \left(\frac{V_l}{V_b} \right)^{1/2} \right]$$
$$= P_0 \exp \left[-7.62l(l+1)/(A_r r_{nf} Z_1 Z_2)^{1/2} \right], \qquad 1.34$$

where r_{nf} is the nuclear radius in units of 1 fermi $= 10^{-15}$ cm. Equation 1.34 confirms that angular momentum components with $l > 0$ have penetration factors much smaller than the $l = 0$ component. This allows us to keep the S-wave term only in the cross-section expansion 1.22, which leads us to evaluate the barrier transparency and the cross section as

$$\mathcal{T} \simeq \mathcal{T}_0 = \left(\frac{V_b}{U_0}\right)^{1/2} \exp\left(-\sqrt{\frac{\epsilon_G}{\epsilon}}\right) \qquad 1.35$$

and

S-wave cross section

$$\sigma(\epsilon) \simeq \sigma_{l=0}(\epsilon) \simeq \left[\pi \frac{\hbar^2}{m_r}\beta_{l=0}\left(\frac{V_b}{U_0}\right)^{1/2}\right]\frac{\exp(-\sqrt{\epsilon_G/\epsilon})}{\epsilon}, \qquad 1.36$$

respectively. Equation 1.36 for the cross section has the same form as the parametrization 1.21, with the term in square brackets corresponding to the astrophysical S-factor.

Another form of eqn 1.35, which will turn useful later, is

$$\mathcal{T} = \left(\frac{V_b}{U_0}\right)^{1/2} \exp\left[-\pi\left(\frac{r_{tp}}{a_B^*}\right)^{1/2}\right], \qquad 1.37$$

where

$$a_B^* = \hbar^2/(2m_r Z_1 Z_2 e^2) \qquad 1.38$$

may be looked at as a nuclear Bohr radius.

1.3 **Some important fusion reactions**

In Table 1.1 we list some fusion reactions of interest to controlled fusion research and to astrophysics. For each reaction the table gives the Q-value, the zero-energy astrophysical factor $S(0)$ and the square root of the Gamow energy ϵ_G. For the cases in which $S(\epsilon)$ is weakly varying these data allow for relatively accurate evaluation of the cross section, using eqn 1.21, with $S = S(0)$.

For some of the main reactions, Table 1.2 gives the measured cross-sections at $\epsilon = 10$ keV and $\epsilon = 100$ keV, as well as the maximum value of the cross-section σ_{max}, and the energy ϵ_{max} at which the maximum occurs. Also shown, in parentheses, are theoretical data for the pp and CC reactions. In the tables and in the following discussion, the reactions are grouped according to the field of interest.

A large and continuously updated database on fusion reactions, quoting original references for all included data, has been produced and is

Table 1.1 Some important fusion reactions and parameters of the cross-section factorization 1.21.

	Q (MeV)	$\langle Q_\nu \rangle$ (MeV)	$S(0)$ (keV barn)	$\epsilon_G^{1/2}$ (keV$^{1/2}$)
Main controlled fusion fuels				
$D + T \rightarrow \alpha + n$	17.59		1.2×10^4	34.38
$D + D \rightarrow$ $T + p$	4.04		56	31.40
$\qquad\qquad$ $^3He + n$	3.27		54	31.40
$\qquad\qquad$ $\alpha + \gamma$	23.85		4.2×10^{-3}	31.40
$T + T \rightarrow \alpha + 2n$	11.33		138	38.45
Advanced fusion fuels				
$D + {}^3He \rightarrow \alpha + p$	18.35		5.9×10^3	68.75
$p + {}^6Li \rightarrow \alpha + {}^3He$	4.02		5.5×10^3	87.20
$p + {}^7Li \rightarrow 2\alpha$	17.35		80	88.11
$p + {}^{11}B \rightarrow 3\alpha$	8.68		2×10^5	150.3
The p–p cycle				
$p + p \rightarrow D + e^+ + \nu$	1.44	0.27	4.0×10^{-22}	22.20
$D + p \rightarrow {}^3He + \gamma$	5.49		2.5×10^{-4}	25.64
$^3He + {}^3He \rightarrow \alpha + 2p$	12.86		5.4×10^3	153.8
CNO cycle				
$p + {}^{12}C \rightarrow {}^{13}N + \gamma$	1.94		1.34	181.0
$[{}^{13}N \rightarrow {}^{13}C + e^+ + \nu + \gamma]$	2.22	0.71	—	—
$p + {}^{13}C \rightarrow {}^{14}N + \gamma$	7.55		7.6	181.5
$p + {}^{14}N \rightarrow {}^{15}O + \gamma$	7.29		3.5	212.3
$[{}^{15}O \rightarrow {}^{15}N + e^+ + \nu + \gamma]$	2.76	1.00	—	—
$p + {}^{15}N \rightarrow {}^{12}C + \alpha$	4.97		6.75×10^4	212.8
Carbon burn				
$^{12}C + {}^{12}C \rightarrow$ $^{23}Na + p$	2.24			
$\qquad\qquad$ $^{20}Na + \alpha$	4.62		8.83×10^{19}	2769
$\qquad\qquad$ $^{24}Mg + \gamma$	13.93			

The Q value includes both positron disintegration energy and neutrino energy, when relevant. The quantity $\langle Q_\nu \rangle$ is the average neutrino energy. As usual in nuclear physics, cross sections are expressed in barn; 1 barn $= 10^{-24}$ cm^2.

updated by the NACRE (Nuclear Astrophysics Compilation of REaction rates) group (Angulo *et al*. 1999) and can also be accessed through the internet.[1] Standard references for fusion reaction rates are a compilation of data by Fowler *et al*. (1967) and its subsequent updates (Fowler *et al*. 1975; Harris *et al*. 1983). Data on many fusion reactions of astrophysical relevance have been recently reviewed by Adelberger *et al*. (1998). Data on the DD, DT, and D ^{3}He reactions have been critically reviewed by Bosch and Hale (1992); the most recent reference on p ^{11}B is Nevins and Swain (2000). An interesting list of thermonuclear reactions has also been published by Cox *et al*. (1990). Graphs of the cross section of reactions of interest to fusion energy versus center-of-mass energy are shown in Fig. 1.3.

[1] See the url address http://pntpm.ulb.ac.be/nacre.htm

Table 1.2 Fusion reactions: cross sections at centre-of-mass energy of 10 keV and 100 keV, maximum cross-section σ_{max} and location of the maximum ϵ_{max}. Values in parentheses are estimated theoretically; all others are measured data.

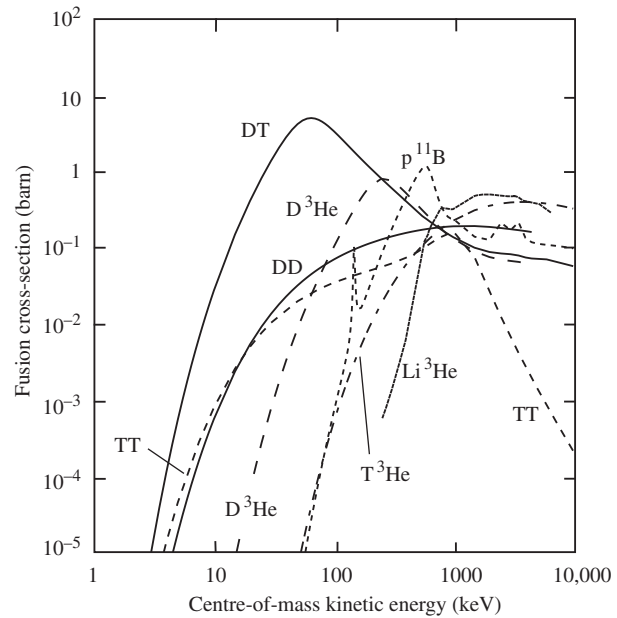| Reaction	σ (10 keV) (barn)	σ (100 keV) (barn)	σ_{max} (barn)	ϵ_{max} (keV)
$D + T \rightarrow \alpha + n$	2.72×10^{-2}	3.43	5.0	64
$D + D \rightarrow T + p$	2.81×10^{-4}	3.3×10^{-2}	0.096	1250
$D + D \rightarrow {}^3He + n$	2.78×10^{-4}	3.7×10^{-2}	0.11	1750
$T + T \rightarrow \alpha + 2n$	7.90×10^{-4}	3.4×10^{-2}	0.16	1000
$D + {}^3He \rightarrow \alpha + p$	2.2×10^{-7}	0.1	0.9	250
$p + {}^6Li \rightarrow \alpha + {}^3He$	6×10^{-10}	7×10^{-3}	0.22	1500
$p + {}^{11}B \rightarrow 3\alpha$	(4.6×10^{-17})	3×10^{-4}	1.2	550
$p + p \rightarrow D + e^+ + \nu$	(3.6×10^{-26})	(4.4×10^{-25})		
$p + {}^{12}C \rightarrow {}^{13}N + \gamma$	(1.9×10^{-26})	2.0×10^{-10}	1.0×10^{-4}	400
${}^{12}C + {}^{12}C$ (all branches)		(5.0×10^{-103})		

Fig. 1.3 Fusion cross sections versus centre-of-mass energy for reactions of interest to controlled fusion energy. The curve labelled DD represents the sum of the cross sections of the various branches of the reaction.
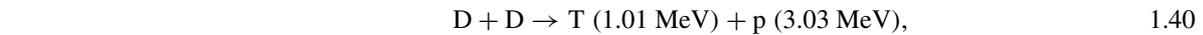
1.3.1   Main controlled fusion fuels

First, we consider the reactions between the hydrogen isotopes deuterium and tritium, which are most important for controlled fusion research. Due to $Z = 1$, these hydrogen reactions have relatively small values of ϵ_G and hence relatively large tunnel penetrability. They also have a relatively large S.

The DT reaction

DT reaction

$$D + T \rightarrow \alpha \ (3.5 \ \text{MeV}) + n \ (14.1 \ \text{MeV}) \qquad 1.39$$
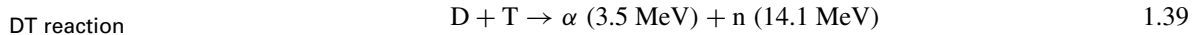
has the largest cross-section, which reaches its maximum (about 5 barn) at the relatively modest energy of 64 keV (see Fig. 1.3). Its $Q_{\text{DT}} = 17.6$ MeV is the largest of this family of reactions. It is to be observed that the cross section of this reaction is characterized by a broad resonance for the formation of the compound ^{5}He nucleus at $\epsilon \cong 64$ keV. Therefore, the astrophysical factor S exhibits a large variation in the energy interval of interest.

The DD reactions

DD reactions

$$D + D \rightarrow T \ (1.01 \ \text{MeV}) + p \ (3.03 \ \text{MeV}), \qquad 1.40$$

$$D + D \rightarrow {}^3\text{He} \ (0.82 \ \text{MeV}) + n \ (2.45 \ \text{MeV}) \qquad 1.41$$

are nearly equiprobable. In the 10–100 keV energy interval, the cross sections for each of them are about 100 times smaller than for DT. The reaction $D(d, \gamma)^4$He, instead has cross section about 10,000 times smaller than that of 1.40 and 1.41.

The TT reaction

TT reaction

$$T + T \rightarrow \alpha + 2n + 11.3 \ \text{MeV}, \qquad 1.42$$
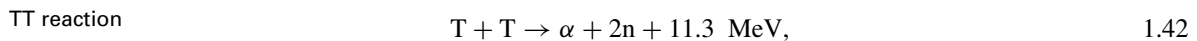
has cross section comparable to that of DD. Notice that since the reaction has three products, the energies associated to each of them are not uniquely determined by conservation laws.

1.3.2   Advanced fusion fuels

Next, we consider reactions between hydrogen isotopes and light nuclei (Helium, Lithium, Boron). In the context of controlled fusion research mixtures of hydrogen and such elements are called *advanced fusion fuels* (Dawson 1981). For this group of reactions the Gamow energy is higher than for the previous group, leading to smaller cross-sections at relatively low energy. At high energy the cross sections are intermediate between that of DD and that of DT.

The proton–boron reaction

p ^{11}B reaction

$$p + {}^{11}\text{B} \rightarrow 3\alpha + 8.6 \ \text{MeV}, \qquad 1.43$$
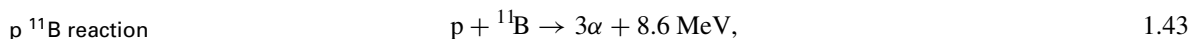
is particularly interesting, because it does not involve any radioactive fuel, and only releases charged particles. Its cross section exhibits a very narrow resonance at $\epsilon = 148$ keV, where the S factor peaks at 3500 MeV·barn and a broader resonance at $\epsilon = 580$ keV, where $S \approx 380$ MeV·barn.

The D ^{3}He reaction also does not involve radioactive fuel and does not release neutrons, but a D ^{3}He fuel would anyhow produce tritium and emit neutrons due to unavoidable DD reactions.

1.3.3   p–p cycle

Reactions involved in the p–p cycle, the main source of energy in the Sun, are of fundamental importance in astrophysics. The first two reactions of the cycle, the pp reaction and the pD reaction have the lowest Gamow energy ϵ_G of all fusion reactions, but their cross sections are much smaller than those of the previous reactions. Indeed, the pp reaction involves a low probability beta-decay, resulting in a value of S about 25 orders of magnitude smaller than that of the DT reaction. The pD reaction involves an electromagnetic transition, which is much more probable than pp, but still much less probable than reactions 1.39–1.43 based on strong interaction.

1.3.4   CNO cycle

Next, Table 1.1 considers the reactions of the CNO cycle, the other main cycle responsible for energy production and hydrogen burning in stars. Here the S factors are not very small, but the Gamow energy takes values close to 40 MeV, thus resulting in cross sections smaller than those of the p–p cycle at relatively low temperatures. Indeed the p–p chain dominates in the Sun, which has central temperature of 1.3 keV (see Bahcall *et al.* 2001). The CNO cycle, instead, prevails over the p–p cycle at temperatures larger than about 1.5 keV.

1.3.5   CC reactions

Finally, Table 1.1 lists data for the reactions between ^{12}C nuclei. Such nuclei are the main constituents of some white dwarfs. It is seen that the S factor is very large, but even at an energy of 100 keV the cross section is below 10^{-100} cm^2, due to the extremely high Coulomb barrier. We shall see in Section 1.5.3 that CC reactions become in fact possible in white dwarfs at densities above 10^9 g/cm^3.

1.4   Maxwell-averaged fusion reactivities

As we have seen earlier, the effectiveness of a fusion fuel is characterized by its reactivity $\langle \sigma v \rangle$. Both in controlled fusion and in astrophysics we usually deal with mixtures of nuclei of different species, in thermal equilibrium, characterized by Maxwellian velocity distributions

$$f_j(v_j) = \left(\frac{m_j}{2\pi k_B T} \right)^{3/2} \exp\left(-\frac{m_j v_j^2}{2k_B T} \right), \qquad 1.44$$

where the subscript j labels the species, T is the temperature and k_B is Boltzmann constant. The expression for the average reactivity 1.10 can

now be written as

$$\langle \sigma v \rangle = \iint d\mathbf{v}_1 \, d\mathbf{v}_2 \, \sigma_{1,2}(v) v f_1(v_1), \qquad 1.45$$

where $v = |\mathbf{v}_1 - \mathbf{v}_2|$ and the integrals are taken over the three-dimensional velocity space. In order to put eqn 1.45 in a form suitable for integration, we express the velocities $\mathbf{v}_1$ and $\mathbf{v}_2$ by means of the relative velocity and of the center-of-mass velocity $\mathbf{v}_c = (m_1\mathbf{v}_1 + m_2\mathbf{v}_2)/(m_1 + m_2)$:

$$\mathbf{v}_1 = \mathbf{v}_c + \mathbf{v}m_2/(m_1 + m_2); \qquad 1.46$$

$$\mathbf{v}_2 = \mathbf{v}_c - \mathbf{v}m_1/(m_1 + m_2). \qquad 1.47$$

Equation 1.45 then becomes

$$\langle \sigma v \rangle = \frac{(m_1 m_2)^{3/2}}{(2\pi k_B T)^3}$$
$$\times \iint d\mathbf{v}_1 \, d\mathbf{v}_2 \exp\left(-\frac{(m_1 + m_2)\mathbf{v}_c^2}{2k_B T} - \frac{m_r v^2}{2k_B T}\right)\sigma(v)v, \quad 1.48$$

where m_r is the reduced mass defined by eqn 1.8, and the subscripts '1,2' have been omitted. It can be shown (see, for example, Clayton 1983) that the integral over $d\mathbf{v}_1 \, d\mathbf{v}_2$ can be replaced by an integral over $d\mathbf{v}_c \, d\mathbf{v}$, so that we can write

$$\langle \sigma v \rangle = \left[\left(\frac{m_1 + m_2}{2\pi k_B T}\right)^{3/2} \int d\mathbf{v}_c \exp\left(-\frac{(m_1 + m_2)}{2k_B T}\mathbf{v}_c^2\right) \right]$$
$$\times \left(\frac{m_r}{2\pi k_B T}\right)^{3/2} \int d\mathbf{v} \exp\left(-\frac{m_r}{2k_B T}\mathbf{v}^2\right)\sigma(v)v. \qquad 1.49$$

The term in square brackets is unity, being the integral of a normalized Maxwellian, and we are left with the integral over the relative velocity. By writing the volume element in velocity space as $d\mathbf{v} = 4\pi v^2 \, dv$, and using the definition 1.7 of center-of-mass energy ϵ, we finally get

$$\langle \sigma v \rangle = \frac{4\pi}{(2\pi m_r)^{1/2}} \frac{1}{(k_B T)^{3/2}} \int_0^\infty \sigma(\epsilon) \, \epsilon \, \exp(-\epsilon/k_B T) d\epsilon. \qquad 1.50$$

1.4.1   Gamow form for non-resonant reactions

Useful and enlightening analytical expressions of the reactivity can be obtained by using the simple parametrization 1.21 of the cross-section. In this case the integrand of eqn 1.50 becomes

$$y(\epsilon) = S(\epsilon) \exp\left[-\left(\frac{\epsilon_G}{\epsilon}\right)^{1/2} - \frac{\epsilon}{k_B T}\right] = S(\epsilon)g(\epsilon, k_B T). \qquad 1.51$$

An interesting result is obtained for temperatures $T \ll \epsilon_G$ and stems from the fact that the function $g(\epsilon, k_B T)$ is the product of a decreasing exponential coming from the Maxwellian times an increasing one originating

Fig. 1.4 Gamow peak for DD reactions at $T = 10$ keV: most of the reactivity comes from reaction between nuclei with center-of-mass energy between 15 and 60 keV.
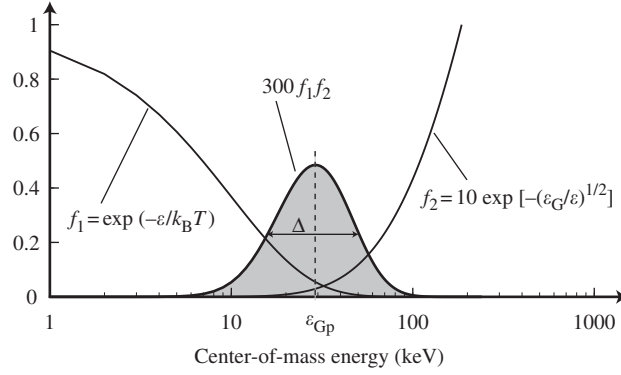
from the barrier penetrability, as shown in Fig. 1.4. It has a maximum at the Gamow peak energy

Gamow peak

$$\epsilon_{Gp} = \left(\frac{\epsilon_G}{4 k_B T} \right)^{1/3} k_B T = \xi k_B T, \qquad 1.52$$

where, for eqn 1.20,

$$\xi = 6.2696 (Z_1 Z_2)^{2/3} A_r^{1/3} T^{-1/3}, \qquad 1.53$$

with the temperature in kiloelectron volt. To perform the integration we use the saddle-point method, that is, we first expand $y(\epsilon)$ in Taylor series around $\epsilon = \epsilon_{Gp}$, thus writing

$$y(\epsilon) \cong S(\epsilon) \exp \left[-3\xi + \left(\frac{\epsilon - \epsilon_{Gp}}{\Delta/2} \right)^2 \right], \qquad 1.54$$

with

$$\Delta = \frac{4}{\sqrt{3}} \xi^{1/2} k_B T. \qquad 1.55$$

Equation 1.54 shows that most of the contribution to the reactivity comes from a relatively narrow energy region with width Δ centered around $\epsilon = \epsilon_{Gp}$, in the high energy portion of the velocity distribution function (see Fig. 1.4)

Using eqns 1.51–1.55 and with the further assumption of non-exponential behaviour of $S(\epsilon)$ we can integrate eqn 1.49 to get the reaction rate in the so-called Gamow form

Gamow reactivity

$$\langle \sigma v \rangle = \frac{8}{\pi \sqrt{3}} \frac{\hbar}{m_r Z_1 Z_2 e^2} \bar{S} \xi^2 \exp(-3\xi). \qquad 1.56$$

Here, we have used $\int_0^\infty \exp(-x^2)\, dx = \sqrt{\pi}/2$, and indicated with $\bar{S}$ an appropriately averaged value of S. In the cases in which S depends weakly on ϵ, one can simply set $\bar{S} = S(0)$. In the following, when distinguishing

between $\bar{S}$ and $S(0)$ is not essential, we shall simply use the symbol S. Improved approximations, taking into account the dependence of S on ϵ are discussed by Clayton (1983) and Bahcall (1966). Inserting the values of the numerical constants eqn 1.56 becomes

$$\langle \sigma v \rangle = \frac{6.4 \times 10^{-18}}{A_{\mathrm{r}} Z_1 Z_2} S \xi^2 \exp(-3\xi) \ \ \mathrm{cm^3/s,} \qquad\qquad 1.57$$

where S is in units of kiloelectron volt barn and ξ is given by eqn 1.53. We remark that the Gamow form is appropriate for reactions which do not exhibit resonances in the relevant energy range. In particular, it is a good approximation for the DD reactivity, while it is not adequate for the DT and D ^{3}He reactions.

Equation 1.57 can be used to appreciate the low-temperature behaviour of the reactivity. By differentiation we get

$$\frac{d\langle \sigma v \rangle}{\langle \sigma v \rangle} = -\frac{2}{3} + \xi \frac{dT}{T}, \qquad\qquad 1.58$$

which leads to

$$\langle \sigma v \rangle \propto T^{\xi} \qquad\qquad 1.59$$

when $\xi \gg 1$. A strong temperature dependence is then found when $T \ll 6.27 Z_1^2 Z_2^2 A_{\mathrm{r}}$, making apparent the existence of temperature thresholds for fusion burn, which are increasing functions of the mass of the participating nuclei.

1.4.2   Reactivity of resonant reactions

When a reaction exhibits a resonance in the energy interval of interest, the astrophysical S factor appearing in the parametrization 1.21 is a strongly varying factor of energy. As a consequence, the reactivity cannot be expressed in the Gamow form 1.56. For a reaction with a single resonance at energy ϵ_{r} we can instead use the Breit–Wigner form of the cross section (see, for example, Segrè 1964, Chapter 11; Burcham 1973, Chapter 15; Blatt and Weisskopf 1953, Chapter VIII)

Breit-Wigner cross section

$$\sigma \propto \lambdabar^2 \frac{\Gamma_a \Gamma_b}{(\epsilon - \epsilon_{\mathrm{r}})^2 + (\Gamma/2)^2}, \qquad\qquad 1.60$$

where Γ is the width of the resonance and Γ_a and Γ_b are the so-called partial widths for the input and the output reaction channels. When Γ is sufficiently small, the cross section takes large values in a narrow energy range centered around $\epsilon = \epsilon_{\mathrm{r}}$. In this interval the channel widths can be taken as constants. The relevant Maxwellian reactivity can then be simply evaluated by assuming that only nuclei with energy falling in the

resonance peak contribute to it. We thus have

$$\langle \sigma v \rangle \simeq \sigma(\epsilon_r) f(\epsilon_r) v_r \frac{\Gamma}{2} \propto T^{-3/2} \exp\left(-\frac{\epsilon_r}{T}\right), \qquad 1.61$$

where $f(v)$ is the relevant Maxwellian velocity distribution function and $v_r = (2\epsilon_r/m_r)^{1/2}$.

1.4.3   Reactivities for controlled fusion fuels

Curves of the reactivity as a function of the temperature, obtained by numerical integration of eqn 1.49 with the best available cross-sections, are shown in Fig. 1.5 for the reactions of interest to controlled fusion. We see that the DT reaction has the largest reactivity in the whole temperature interval below 400 keV. The DT reactivity has a broad maximum at about 64 keV; it is 100 times larger than that of any other reaction at 10–20 keV and 10 times larger at 50 keV. The second most probable reaction is DD at temperatures $T < 25$ keV, while it is $D\,^3He$ for $25 < T < 250$ keV. The reactivity of $p\,^{11}B$ equals that of $D\,^3He$ at temperature about 250 keV and that of DT at about 400 keV. At such very high temperatures other reactions (such as $T\,^3He$, $p\,^9Be$, $D\,^6Li$) have reactivity comparable to that of $p\,^{11}B$, but they are less interesting for controlled fusion because the fuels involved either contain rare isotopes or generate radioactivity (Dawson 1981).

In the range of temperatures 1–100 keV the reactivity of the DT, DD, and $D\,^3He$ reactions are accurately fitted by the functional form
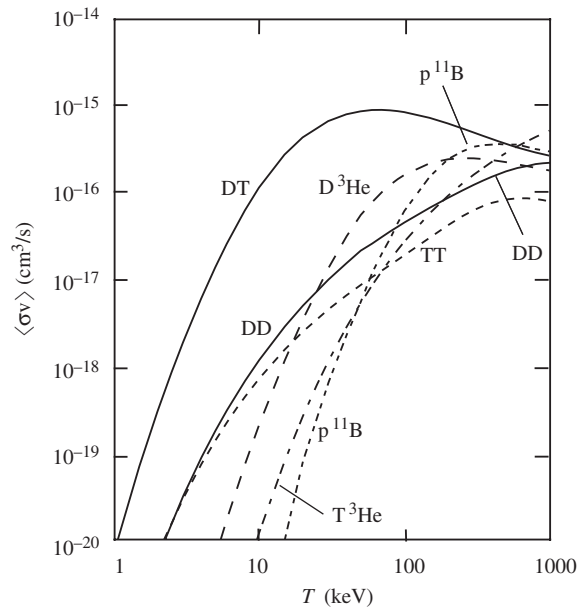
DT has the largest reactivity

Fig. 1.5   Maxwell-averaged reaction reactivity versus temperature for reactions of interest to controlled fusion.

(Bosch and Hale 1992)

Accurate reactivity fit

$$\langle \sigma v \rangle = C_1 \zeta^{-5/6} \xi^2 \exp(-3\zeta^{1/3}\xi) \qquad\qquad 1.62$$

where

$$\zeta = 1 - \frac{C_2 T + C_4 T^2 + C_6 T^3}{1 + C_3 T + C_5 T^2 + C_7 T^3} \qquad\qquad 1.63$$

and ξ is given by eqn 8.97, which can be written as

$$\xi = C_0/T^{1/3}. \qquad\qquad 1.64$$

It is seen that the Gamow form 1.57 is recovered as the temperature $T \to 0$, and then $\zeta \to 1$. At high temperatures the assumed functional form allows for including reactions occurring in the wing of a resonance. The values of the constant C_0 and of the fit coefficients C_1–C_7 appearing in eqns 1.62–1.64 are listed in Table 1.3. The table also gives estimated errors of the fit.

The reactivity of the p ^{11}B reaction, instead, is well fitted by the expression (Nevins and Swain 2000)

$$\langle \sigma v \rangle_{pB} = C_1 \zeta^{-5/6} \xi^2 \exp(-3\zeta^{1/3}\xi) + 5.41 \times 10^{-15} T^{-3/2}$$
$$\times \exp(-148/T) \ \text{cm}^3/\text{s}, \qquad\qquad 1.65$$

with ζ still given by eqn 1.63, and the values of the coefficients C_0–C_7 listed in Table 1.3. The second term on the right-hand side of eqn 1.65 accounts for the previously mentioned narrow resonance at 148 keV, and has the functional form 1.61. In eqn 1.65 and in the following eqns 1.66–1.71 the temperature T is in units of kiloelectron volt.

Table 1.3 Parameters for the reactivity fit, eqns 1.62–1.65; here energies and temperatures are in keV, and the reactivity in cm^3/s. The compact notation $A(b,c)D$ used here stands, as usual, for $A + B \to C + D$.

Reaction Fit (eqn number)		T(d, n)α 1.62	D(d, p)T 1.62	D(d, n)^{3}He 1.62	^{3}He(d, p)α 1.62	^{11}B(p, α)2α 1.65
C_0	keV$^{1/3}$	6.6610	6.2696	6.2696	10.572	17.708
$C_1 \times 10^{16}$	cm^3/s	643.41	3.7212	3.5741	151.16	6382
$C_2 \times 10^3$	keV^{-1}	15.136	3.4127	5.8577	6.4192	−59.357
$C_3 \times 10^3$	keV^{-1}	75.189	1.9917	7.6822	−2.0290	201.65
$C_4 \times 10^3$	keV^{-2}	4.6064	0	0	−0.019108	1.0404
$C_5 \times 10^3$	keV^{-2}	13.500	0.010506	−0.002964	0.13578	2.7621
$C_6 \times 10^3$	keV^{-3}	−0.10675	0	0	0	−0.0091653
$C_7 \times 10^3$	keV^{-3}	0.01366	0	0	0	0.00098305
T range	keV	0.2–100	0.2–100	0.2–100	0.5–190	50–500
Error		<0.25%	<0.35%	<0.3%	<2.5%	<1.5%

Simpler formulas are useful for rapid evaluations. For the DT reaction, which is by far the most important one for present fusion research, the expression (Hively 1983)

Useful reactivity expressions

$$\langle \sigma v \rangle_{\text{DT}} = 9.10 \times 10^{-16} \exp\left(-0.572 \left| \ln \frac{T}{64.2} \right|^{2.13}\right) \text{ cm}^3/\text{s}, \qquad 1.66$$

is 10% accurate in the range 3–100 keV, and 20% accurate in the range 0.3–3 keV. Power law expressions can be useful in analytic studies. In particular, in the temperature range 8–25 keV the DT reactivity is approximated to within 15% by

$$\langle \sigma v \rangle_{\text{DT}} = 1.1 \times 10^{-18} \, T^2 \text{ cm}^3/\text{s}. \qquad 1.67$$

For the two main branches of the DD reaction good approximations are provided by slightly modified Gamow expressions (Hively 1977):

$$\langle \sigma v \rangle_{\text{DDp}} = 2 \times 10^{-14} \frac{1 + 0.00577 T^{0.949}}{T^{2/3}} \exp\left(-\frac{19.31}{T^{1/3}}\right) \text{cm}^3/\text{s} \quad 1.68$$

and

$$\langle \sigma v \rangle_{\text{DDn}} = 2.72 \times 10^{-14} \frac{1 + 0.00539 T^{0.917}}{T^{2/3}} \exp\left(-\frac{19.80}{T^{1/3}}\right) \text{ cm}^3/\text{s}. \qquad 1.69$$

Here the subscripts DDp and DDn indicate the reaction branches 1.40 and 1.41, releasing a proton and a neutron, respectively. Equations 1.68 and 1.69 are about 10% accurate in the temperature range 3–100 keV.

For the D ^{3}He reactions one can use the expression (Hively 1983)

$$\langle \sigma v \rangle_{\text{D}^3\text{He}} = 4.98 \times 10^{-16} \exp\left(-0.152 \left| \ln \frac{T}{802.6} \right|^{2.65}\right) \text{ cm}^3/\text{s}, \qquad 1.70$$

which is 10% accurate for temperatures in the range 0.5–100 keV.

It is interesting to compare the above reactivities to that of the pp reaction (Angulo *et al*. 1999)

$$\langle \sigma v \rangle_{\text{pp}} = 1.56 \times 10^{-37} T^{-2/3} \exp\left(-\frac{14.94}{T^{1/3}}\right)$$
$$\times (1 + 0.044 T + 2.03 \times 10^{-4} T^2 + 5 \times 10^{-7} T^3) \text{ cm}^3/\text{s}. \qquad 1.71$$

We immediately find that the pp reactivity is 24–25 orders of magnitude smaller than that of DT at temperatures of 1–10 keV. It may be surprising to observe that the specific power of fusion reactions at the center of the Sun takes the very small value of 0.018 W/kg, that is, about 1/50 the metabolic heat of the human body!

1.5 Fusion reactivity in very high density matter

The previous evaluations of the reactivity assume free ions, with Maxwellian velocity distribution function, and neglect any effect due to the plasma electrons. The reactivities are then only functions of the temperature, and the volumetric reaction rates are proportional to the reactivity times the density squared. In practice this proves adequate for laboratory plasmas. However, other situations occur in nature, or may perhaps even be produced in the laboratory, where high density effects should be taken into account. In this section we give a brief account of the problem; the reader interested in a thorough treatment is referred to specialized texts such as a recent book by Ichimaru (1994).

Thermonuclear reactions

We have seen in the previous section that when the reacting nuclei have Maxwell distribution with $0.1 \geq T \geq 100$ keV, then most of the reactivity comes from hot nuclei with energy $\epsilon \approx \epsilon_{\mathrm{Gp}} \gg k_{\mathrm{B}}T$. This justifies the usual name of thermonuclear reactions. In a low density plasma the thermal energy $k_{\mathrm{B}}T$, in turn, exceeds by far the average potential energy, a typical value for which can be $V_{c0} = V_{\mathrm{c}}(a)$, that is, the potential at a distance equal to the average interparticle distance a. In terms of the so-called plasma parameter $\Gamma = Ze^2/ak_{\mathrm{B}}T$ the results of the previous section apply when

Plasma parameter

$$\Gamma \ll 1 \ll \epsilon_{\mathrm{Gp}}/k_{\mathrm{B}}T. \qquad\qquad 1.72$$

At high densities or, more properly, as Γ becomes comparable to unity, nuclear charge screening by the electrons and ion correlation become important. Anyhow, as far as $\epsilon_{\mathrm{Gp}} \gg V_{c0}$, the reactivity will still be dominated by the tail of the ion distribution (i.e. by the hottest ions), and we can still speak of thermonuclear fusion. We show below that such processes result in small corrections to the pp reactivity in the sun, and in practically negligible effects for laboratory inertially confined fuels. In some strongly correlated plasmas the corrections can be large, but apply to vanishingly small reactivities, so that fusion will not occur anyhow.

Pycnonuclear reactions

A new situation, instead, occurs when the density is so large that not only $\Gamma \gg 1$, but also the average potential energy exceeds the Gamow peak energy: now the thermal motion is no more responsible for the majority of the reactions, and the reactivity depends on the density only. For such a regime Cameron (1959) coined the word pycnonuclear fusion (from the Greek $\pi\upsilon\kappa\nu o\sigma$ meaning dense).

An extreme pycnonuclear regime is predicted to occur in crystalline solids at very low temperature, where the ions, frozen in the lattice, perform zero-point quantum mechanical oscillations around their equilibrium position. Pycnonuclear regimes are held responsible for Carbon combustion in highly compressed white-dwarf stars.
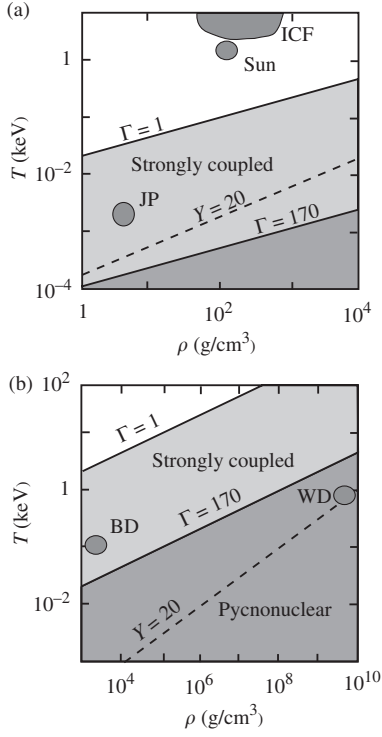
(a)

(b)

Fig. 1.6 Regions in the density–temperature plane where strong coupling and high density effects occur, for (a) hydrogen and (b) carbon. Points representing inertially confined burning DT plasmas (ICF), the center of the Sun, the centre of Jovian planets (JP), brown dwarfs (BD), and white dwarfs (WD) are also shown.

In the next subsections, we summarize the main results of detailed treatments concerning weakly electron screened plasma ($\Gamma < 1; \epsilon_{\text{Gp}} \gg V_{c0}$), strongly coupled plasma ($1 < \Gamma < 170; \epsilon_{\text{Gp}} > V_{c0}$), and crystalline lattice ($\Gamma > 170$), respectively. The regions in the density–temperature plane, corresponding to the above cases are shown in Fig. 1.6 for hydrogen and carbon plasmas. There, conditions representative of inertial confinement fusion (ICF) fuels, sun interior, white dwarfs, brown dwarfs, and giant planets are also indicated. It is apparent that the interior of the Sun and ICF plasmas are only marginally related to dense plasma effects, which can instead be important for planetary interiors and white dwarfs.

In this section, we deal with the so-called static screening, that is, the screening computed considering test particles with energy equal to the mean ion energy $k_{\text{B}}T$. For completeness, we mention that some authors have studied possible dynamic screening effects, that is, effects related to a difference between the potential felt by a test particle with energy about the Gamow energy, and the potential felt by a plasma ion, in statistical equilibrium, with the same kinetic energy. The issue of the relevance of dynamical effects is still debated; see, for example, the recent reviews by Brown and Sawyer (1997) and Shaviv and Shaviv (1999).

1.5.1 Electron screened, weakly coupled plasmas

According to the classical theory of plasmas, which applies for $\Gamma \ll 1$, each particle only feels the effect of the particles at a distance smaller than the Debye length λ_{D} (see Section 11.1), while on longer scales the plasma is quasi-neutral. A good approximation to the potential energy of a nucleus at distance r from another nucleus is given by

$$V_{\text{eff}}(r) = V_{\text{c}}(r) \exp(-r/\lambda_{\text{D}}),   \qquad 1.73$$

where the factor $\exp(-r/\lambda_{\text{D}})$ accounts for the screening effects of the electrons. The effective potential barrier to be tunnelled in a fusion reaction can then be approximated as

$$V(r) = \frac{Z_1 Z_2 e^2}{r} \exp(-r/\lambda_{\text{D}}) \approx \frac{Z_1 Z_2 e^2}{r} - \frac{Z_1 Z_2 e^2}{\lambda_{\text{D}}} = V_{\text{c}}(r) - \epsilon_s,$$

$$1.74$$

where $\epsilon_s = Z_1 Z_2 e^2/\lambda_{\text{D}}$. By using the WKB approximation (see Section 1.2.3) we find that the barrier transparency takes the same form as eqn 1.35, once the energy ϵ is replaced by $\epsilon' = \epsilon + \epsilon_s$. Consequently, the energy of the Gamow peak shifts to a smaller value $\epsilon_{\text{Gps}} = \epsilon_{\text{Gp}} - \epsilon_s$; the width of the Gamow peak is left unchanged, while the maximum of the integrand in eqn 1.51 increases by a factor $\exp(\epsilon_s/k_{\text{B}}T) = \exp(\sqrt{3}\Gamma_e^{3/2})$,

where $\Gamma_e = V_c(a_e)/k_B T$ is the plasma parameter at the average inter-electron distance. The reaction rate can then be written as

$$\langle \sigma v \rangle_{\text{es}} \approx A_{\text{se}} \langle \sigma v \rangle \cong (1 + \sqrt{3} \Gamma_e^{3/2}) \langle \sigma v \rangle, \qquad\qquad 1.75$$

where $\langle \sigma v \rangle$ is the value computed by neglecting any screening, and A_{se} the reactivity amplification factor due to the electron screening (Salpeter 1954). A comparable effect is also due to ion correlation (Ichimaru 1994). We now use the above result to evaluate the electron screening corrections in two interesting cases. At the center of the Sun $\rho \approx 130$ g/cm^3, $T = 1.5$ keV, and then $A_{\text{se}} = 1.014$. In a deuterium–tritium ICF plasma at ignition, $\rho \approx 100$ g/cm^3, $T = 5$ keV, and then $A_{\text{se}} = 1.002$.

Screening marginal for Sun and ICF

1.5.2 Strongly coupled plasma

As Γ approaches unity or becomes even larger than unity, the screened field observed by a nucleus is no more approximated by eqn 1.73; in addition, ion correlation becomes important. The accurate treatment requires using advanced statistical plasma theory (Ichimaru 1994). On a simple heuristic basis, confirmed by the appropriate calculations, we can still approximate electron screening by an expression of the same form as eqn 1.73, and replace the Debye length with the interparticle distance a. Under the condition $\epsilon_{\text{Gp}} > k_B T$, we get a correction A_{se} to the reactivity due to electron screening, of the order of $A_{\text{se}} \approx \exp \Gamma_e$. An analogous, and usually numerically comparable, correction is due to ion screening. Also ion correlation results in increased reactivities, by a factor roughly estimated as $A_i = \exp(\Gamma_i)$, where Γ_i is the plasma parameter at the average inter-ion distance.

The corrections to the reactivities just discussed are large, but concern plasmas at low temperature, since $T(\text{keV}) \simeq 0.02 Z_1 Z_2 [\rho(\text{g/cm}^3)]^{1/3} / \Gamma_i$. Therefore they only affect reactivities, which are too small to be of any practical interest both to fusion research and to astrophysics or geophysics.

1.5.3 Crystalline solids: pycnonuclear limit

When $\Gamma_i > 170$, each ion is frozen in a crystalline lattice and oscillates with frequency ω around its equilibrium position. A limiting case occurs when the energy $\epsilon_0 = (4\pi n_i Z^2 e^2 / 3 m_i)^{1/2}$ of the ground state of such quantum-mechanical oscillators exceeds considerably the ion thermal energy (i.e. when $Y = \epsilon_0 / k_B T > 20$), here Z, m_i, and n_i are, respectively, the ion charge, mass, and number density. In this case, each nucleus only performs small amplitude oscillations proportional to the interparticle distance $a \propto \rho^{-1/3}$, and can only interact with the nuclei in the neighbouring lattice position; according to eqn 1.37, the dominating exponential factor in the barrier transparency scales as $G \propto r_{\text{tp}}^{1/2} \propto a^{1/2} \propto \rho^{-1/6}$. The transparency is then proportional

to $\exp(-\rho^{1/6})$, without any dependence on temperature. Accurate computations of the CC reactivity at $\Gamma_i > 170$ and $Y > 20$ confirm this behaviour, giving the result $\langle\sigma v\rangle_{CC} = 10^7 \rho_8^{-0.6} \exp\left(-258\rho_8^{-1/6}\right)$ cm^3/s, where ρ_8 is the density in units of 10^{-8} g/cm^3 (Salpeter and Van Horn 1969; Ichimaru 1994). This expression can be improved to account for the finite value of the temperature (Ichimaru 1994; sec. 5.3.D). This pycnonuclear regime is held responsible for sudden power release by very dense and relatively cold white dwarfs with a carbon core. When this core is compressed to density about 10^9 g/cm^3 the reactivity increases rapidly approaching the value it would take at very high temperature and low density, thus igniting carbon combustion.

Carbon burn in white dwarfs

1.6 — Spin polarization of reacting nuclei

In the previous section we have discussed how the fusion rate is affected by condensed-matter effects which modify the Coulomb potential or alter the motion of the interacting nuclei, but do not affect the intrinsic features of the nuclear fusion process. For some reactions it is instead possible to act on the nuclear factor S by using spin-polarized fuels. We refer, for example, to the DT reaction for which the effect is better understood; similar arguments also apply to D ^{3}He.

The DT reaction occurs through formation of a compound ^{5}He nucleus; in about 99% of the cases the excited state has an energy of 64 keV, even parity Π and angular momentum $J = 3/2$ (in units of $\hbar$). It is found that a colliding DT system with even parity and $J = 3/2$ has a probability to react two orders of magnitude larger than a system with different parity and/or angular momentum. Concerning angular momentum, this is in general obtained by summing (according to the usual quantum mechanics rules) the spins and the angular momenta of the interacting particles. The different allowed configurations have statistical weight $g_J = 2J + 1$. In the present case, according to the discussion of Section 1.2.3, we can restrict attention to systems with $l = 0$. Therefore J is simply the sum of the spins of the D and T reacting nuclei. Since the spin of D is 1 and that of T is 1/2, we then have either $J = 1/2$, with $g_{1/2} = 2$, or $J = 3/2$, with $g_{3/2} = 4$. Consequently, if the nuclei are randomly polarized, virtually all reactions are due to a fraction $g_{3/2}/(g_{3/2} + g_{1/2}) = 2/3$ of all collisions. If, instead one could polarize the fuel, that is, align the spins of both D and T along a given axis, so as to have $J = 3/2$ for all collisions, the cross section would increase by 50%.

DT cross section depends on nuclear spin alignment

The use of spin polarization in controlled fusion experiments has been proposed by Kulsrud *et al.* (1982, 1986). More (1983) discussed its application to ICF. Although its practicability is to be demonstrated, spin polarization should be kept in mind since it offers the potential for

a non-negligible increase in the reactivity. It can also lead to relaxed requirements for fusion ignition.

1.7 μ-catalysed fusion

The reactivities computed in Section 1.4 refer to nuclei which move freely. Since each nucleus 1 can react with each nucleus 2, the volumetric reaction rate is then proportional to the product of the densities of the reacting species. The reactivity of nuclei bound in a diatomic molecule has to be computed in a different way. In this case, the volumetric reaction rate R is given by the product of the density n of the molecules, times the probability ν of reaction per molecule per unit time. The latter is proportional to a characteristic constant A_s, only depending on the reacting nuclei, times the square of the wave function for zero separation of the reaction partners:

$$R = n\nu = n A_s \left| \psi(0) \right|^2 . \qquad 1.76$$

It can be shown that A_s is related to the astrophysical factor S by $A_s = S/\pi \alpha_f c m_r$. The wavefunction $\psi(0)$ is computed by solving the Schroedinger equation for the appropriate potential; the dominant exponential factor can be estimated by the WKB tunnelling integral.

The above reactivity applies, in particular to a molecule of hydrogen isotopes, at room temperature. The binding electrons generate an attractive potential (see, for example, Schiff 1968), such that the equilibrium distance of the nuclei is of the order of the Bohr radius

$$a_B = \frac{\hbar^2}{m_e e^2} = 0.529 \times 10^{-8} \, \text{cm}. \qquad 1.77$$

(More precisely, the distance of the hydrogen nuclei is 0.74×10^{-8} cm.) As the nuclei approach at distance $r \ll r_c$ they just feel the repulsive Coulomb potential 1.13. The fusion reaction rate of a deuterium molecule has been computed by Van Sieclen and Jones (1986), using eqn 1.76. It turns out that the reaction frequency is $\nu = w^{-1} \approx 10^{-63} \text{s}^{-1}$, so that the reaction time τ_f is practically infinite even on cosmological scales. Indeed, according to eqn 1.37 the corresponding barrier transparency can be written as

Fusion reactions in a D$_2$ molecule

$$\mathcal{T} \approx \exp\left[-2\sqrt{2Z_1 Z_2} \left(\frac{r_{tp}}{a_B} \frac{m_r}{m_e} \right)^{1/2} \right], \qquad 1.78$$

where m_r is the reduced mass of the two-nuclei system, and we have neglected the front factor $(V_b/U_0)^{1/2}$ in eqn 1.37. For DD reactions in a D_2 molecule, and taking $r_{tp} = a_B$, we get the extremely small value $\mathcal{T} \approx \exp(-121) = 3 \times 10^{-53}$.

According to eqn 1.78, the tunnelling factor and hence the reaction rate, could be increased by reducing the equilibrium distance a_B, and eqn 1.77 shows that a_B is inversely proportional to the mass of the negatively charged particle binding the molecule. In 1947, Frank (1947) and Sacharov (see Sacharov 1989) independently suggested that nuclear fusion occurs with high probability in pseudo-molecules or pseudo-ions bound by a μ meson or muon, which has the same charge $-e$ as the electron and mass $m_\mu = 208 m_e$. It is unstable with a half-life $\tau_\mu = 2.2\ \mu s$. Fusion reactions catalysed by muons were experimentally detected a few years later (Alvarez *et al.* 1957). According to eqn 1.78 the tunnelling factor for nuclei bound in a muonic molecule is about 50 orders of magnitude larger than in an ordinary molecule. In fact, accurate computations show that the advantage is even larger, and one has $\tau_f = 7 \times 10^{-13}$ s for DT reactions in a $D\mu T$ pseudo-molecule and $\tau_f = 1.5 \times 10^{-9}$ s for DD reactions in a $D\mu D$ pseudo-molecule. After the reaction most of the muons are freed and available to catalyse further reactions. One is therefore led to studying the feasibility of energy production by μ-catalysed fusion reactions (Ponomarev 1990; Bertin and Vitale 1992).

For energy production by μ-catalysed fusion, it is necessary that the N_f reactions catalysed on average by one muon release a larger amount of energy than that required to produce the muon itself. The muon is obtained by the decay of the pion, with an estimated cost of 5 GeV. Assuming that fusion energy is converted to electricity with efficiency of 40%, and recalling that a DT reaction releases 17.6 MeV, then reactor self-sustainment demands $N_f > 3000/(17.6 \times 0.4) = 700$. For practical energy production, $N_f > 3000$ is required.

A simplified muon catalysis cycle in a DT mixture is illustrated in Fig. 1.7 [for a detailed discussion, see Bertin and Vitale 1992]. The muon can form either a $T\mu$ or $D\mu$ pseudo-atom; in this last case the μ is transferred to tritium in a time τ_{DT} to form $T\mu$. A $D\mu T$ molecule is then formed in a time $\tau_{DT\mu} \approx 10^{-9}$ s; here, DT fusion occur in a time $\tau_f \approx 7 \times 10^{-13}$ s. After the reaction, most muons are freed, and available again to catalyse fusion reactions. The whole cycle just described occurs in a time $\tau_c \simeq 5 \times 10^{-9}$ s. A small fraction w_s of muons is instead captured by the α-particle and then lost to the cycle. The theoretically predicted value for this sticking probability is $w_s \simeq 0.006$. This leads to estimating $N_f = 1/(w_s + \tau_c/\tau_\mu) \leq 120$, which is not sufficient for energy production. However, in experiments values of N_f up to 200 have been measured, leaving room for improvement. Research in the field has been reviewed by Bertin and Vitale (1992) and Ponomarev (1990). The primary goals of current activities are the understanding of all the individual steps of muon life-cycle, and finding possible ways to reducing cycle time and muon sticking to α-particles.
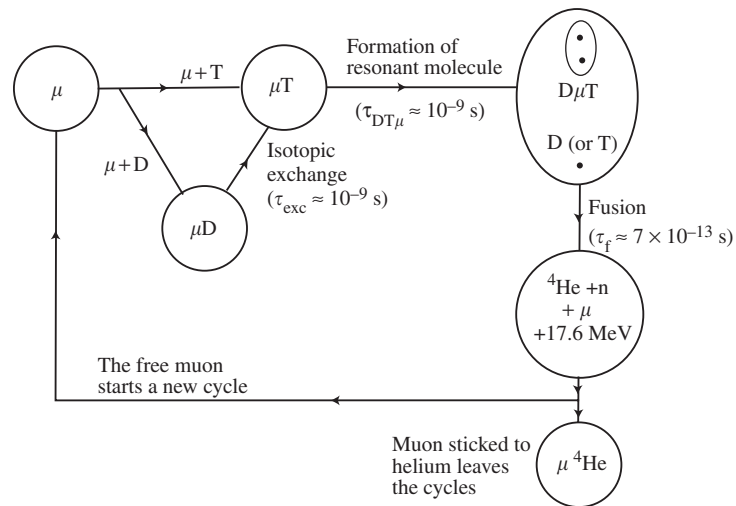
μ-bound molecules and μ-catalysed fusion

Energy production by μ-catalysed fusion

DT μ-catalysis cycle

Fig. 1.7 DT μ-catalysis cycle; mean reaction times are indicated for each process (Bertin and Vitale 1992).

1.8 | **Historical note**

In 1920 Aston found that the mass of the helium nucleus is smaller than four times the mass of the hydrogen atom. Immediately, Eddington (1920a, 1926) observed that the transformation of hydrogen into helium could provide enough power to sustain the sun and, more generally, postulated nuclear reactions as the mechanism powering the stars. However, he was puzzled by the fact that the inferred star temperatures are well below those thought necessary to allow particles to react effectively.

Just at the dawn of wave-mechanics, Gurney and Condon (1929) and, independently, Gamow (1928), computed the probability of tunnelling a barrier. Gamow showed that quantum-mechanical tunnelling explains observations on α-particle decay. In the following year, Atkinson and Houtermans (1929a,b) used Gamow's result to point out that tunnelling opens the way to hydrogen fusion reactions, which could be responsible for the energy production in the stars.

In 1932, Cockcroft and Walton at the Cavendish Laboratory, Cambridge University, directed by Lord Rutherford, were able to produce and detect for the first time a fusion reaction, by bombarding lithium samples with a 100 keV proton beam generated by an accelerator they had designed and built (Cockroft and Walton 1932). In the following 2 years, at the same laboratory, the team led by Lord Rutherford and also including Oliphant, Lewis, Hartweck, Kempton, Shire and Crouther, discovered many other fusion reactions between light elements

and accelerated protons or deuterons (see Chadwick 1965; Oliphant *et al*. 1934a,b).

Deuterium, indeed, had been discovered in 1932 by Urey and coworkers (Urey and Teal 1935), and pure samples were produced in appreciable amounts. A small quantity was soon made available to Cavendish laboratory, and deuterium induced reactions were evidenced. This also led to the discovery, in 1934, of tritium, produced by one of the branches of the DD reaction. Tritium instability, however, was only discovered by Alvarez in 1939.

In 1937 von Weizsäcker proposed the pp reaction chain as the origin of the sun power. Arguments about the insufficiency of the relevant cross-section to account for astronomical observations were put to rest the following year by Bethe and Critchfield (1938), who developed a theory of that reaction, based on the work on β-decay by Fermi and by Gamow and Teller.

Soon later, Bethe (1939) developed the theory of the CNO cycle of energy production in stars. In a few years, with important contributions by Bethe, von Weizsäcker, Gamow, Teller and others, the basics of stellar nucleosynthesis were established. The main reactions were identified, their cross sections approximately computed and the results compared with available data on stellar composition. A classical summary of the achievements of the pioneering stages of nucleosynthesis studies can be found in a famous paper by Burbidge *et al*. (1957).

During wartime, some of the scientist who were developing fission weapons considered the possibility of weapons exploiting fusion reactions. The basis for fusion energy research were also laid down in discussions between Fermi, Teller, Konopinsky, and others. In the same period, the cross sections for the DD reactions were measured rather accurately. A group from Purdue university, probably following a suggestion by Bethe, measured the DT cross-section. To everybody's surprise, it appeared that DT has much larger cross-section than DD in a wide energy range (Diven *et al*. 1983). Such results were only released in 1948 (Hanson *et al*. 1949), after improved measurements had been performed. The theory of the DT reaction was published by Flowers (1950), while treatments of the DD reactions had already appeared in the late 1930s, and were critically reviewed by Konopinski and Teller (1948).

Cross sections for the D-based reactions were accurately measured again in the early fifties (Arnold *et al*. 1954), and one can say that by that time the basic physics of the nuclear fusion reactions of interest to controlled energy production had been established.

Between 1949 and 1955, the cold war efforts led to the development of thermonuclear weapons, the first man made devices to exploit energy released by fusion reactions (see the literature cited in Section 3.5). Research on controlled fusion was initiated in several countries between 1946 and 1950, under strict secret classification. Declassification of these activities occurred about the mid-1950s, when the previous work was

publicly reviewed (Post 1956; Longmire *et al*. 1959). Large fusion pro-
grams where set-up in the main industrial countries and basic books on
plasmas and controlled thermonuclear reactions, which have now become
classics, appeared (Spitzer 1962; Glasstone and Lovberg 1960; Rose and
Clarke 1961; Artsimovich 1964).